Design and Evaluation of a Quasi-Passive Knee Exoskeleton for Investigation of Motor Adaptation in Lower Extremity Joints

Kamran Shamaei*, *Student Member, IEEE*, Massimo Cenciarini, *Member, IEEE*, Albert A. Adams, Karen N. Gregorczyk, Jeffrey M. Schiffman, and Aaron M. Dollar, *Senior Member, IEEE*

Abstract—In this study, we describe the mechanical design and control scheme of a quasi-passive knee exoskeleton intended to investigate the biomechanical behavior of the knee joint during interaction with externally applied impedances. As the human knee behaves much like a linear spring during the stance phase of normal walking gait, the exoskeleton implements a spring across the knee in the weight acceptance (WA) phase of the gait while allowing free motion throughout the rest of the gait cycle, accomplished via an electromechanical clutch. The stiffness of the device is able to be varied by swapping springs, and the timing of engagement/disengagement changed to accommodate different loading profiles. After describing the design and control, we validate the mechanical performance and reliability of the exoskeleton through cyclic testing on a mechanical knee simulator. We then describe a preliminary experiment on three healthy adults to evaluate the functionality of the device on both left and right legs. The kinetic and kinematic analyses of these subjects show that the exoskeleton assistance can partially/fully replace the function of the knee joint and obtain nearly invariant moment and angle profiles for the hip and ankle joints, and the overall knee joint and exoskeleton complex under the applied moments of the exoskeleton versus the control condition, implying that the subjects undergo a considerable amount of motor adaptation in their lower extremities to the exoskeletal impedances, and encouraging more in-depth future experiments with the device.

Index Terms—Knee biomechanics, lower extremity exoskeleton, quasi-passive mechanism, variable-stiffness.
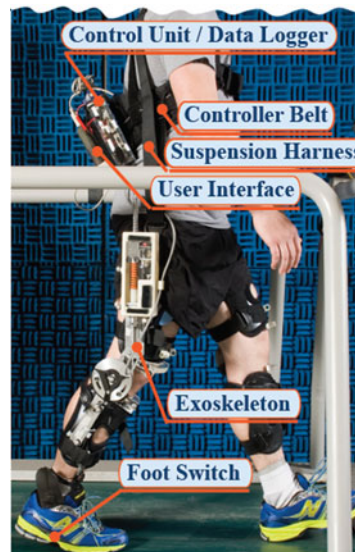

Fig. 1. Quasi-passive knee exoskeletons worn on a volunteer. The control unit is mounted on a belt and wirelessly transfers the data to a host computer. The exoskeletons and controller are supported by a harness from the shoulder.

*K. Shamaei is with the Department of Mechanical Engineering and Materials Science, Yale University, New Haven, CT 06511 USA (e-mail: kamran.shamaei@yale.edu).

M. Cenciarini is with Neurologische Universitätsklinik Freiburg Breisacher Freiburg D-79106, Germany (e-mail: massimo.cenciarini@uniklinik-freiburg.de).

A. A. Adams, K. N. Gregorczyk, and J. M. Schiffman are with the US Army Natick Soldier Research, Development and Engineering Center, Natick, MA 01760 USA (e-mail: albert.a.adams16.civ@mail.mil; karen.n.gregorczyk.civ@mail.mil; jeffrey.m.schiffman.civ@mail.mil).

A. M. Dollar is with the Department of Mechanical Engineering and Materials Science, Yale University, New Haven, CT 06511 USA (e-mail: aaron.dollar@yale.edu).

I. INTRODUCTION

LOWER-EXTREMITY exoskeletons have been actively investigated in the past few decades, with a number of impressive and substantial undertakings (e.g., see [1] for a thorough review). These devices generally intend to augment the locomotion performance of able-bodied users in terms of metabolic cost, load carrying capacity, fatigue, and muscle force generation (in contrast to oftentimes similar lower-limb orthoses intended for impaired subjects [2], [3]). While development efforts have been extensive, lower-limb exoskeleton devices have demonstrated limited success in achieving their augmentation goals [1], [4]–[6], highlighting the challenges in developing artificial systems that can augment the performance of the human body, which is generally substantially more efficient than engineered systems. The lack of successful device development has prompted a number of research efforts intended to investigate basic science questions related to the interaction between lower extremities and wearable robotic devices (e.g., [5], [7]–[11], including the work described in this paper. In order to examine a portion of the many questions related to that interaction, we propose a knee exoskeletal device that can replicate the spring-like behavior of the joint during stance through an external spring

and clutch system that activates and releases via a controller informed by an insole-based footswitch (see Fig. 1). While this device allows for the investigation of how variation in passive impedances affects the gait behavior of the wearer, we believe the approach of carefully tuned external stiffness may eventually prove functional as a performance-augmenting strategy; noting that similar approaches have been proposed and implemented by others [6], [12], [13].

In terms of technical approaches to developing augmenting exoskeletons, engineers have implemented a spectrum of assistance strategies. This includes "sensitivity amplification" [14], "get out of the way" [1], "moment of inertia compensation" [15], pneumatic actuation [16], [17] in fully articulated exoskeletons at one end of the spectrum, and "gravity compensation" in a passive system at the other end [18]. More closely related to the work described in this paper, recent design efforts have focused on replication of the function of lower extremity joints by quasi-passive systems that mostly rely on energy storage/recoil using spring-clutch systems [2], [3], [6], [9], [13], [19]. This approach was inspired by spring-type behavior observed in lower extremity joints during walking and running and proved to lead to lower weight and more functional exoskeletons [11].

In terms of efforts to examine basic science questions related to how a user interacts with a wearable robotic exoskeleton device, a smaller but increasing number of studies have been undertaken to investigate physiological and biomechanical performance of lower extremity joints that interactively function in close proximity to exoskeletal devices [10], [20]–[24]. To this end, researchers have begun to exploit the considerable potential of exoskeletal systems to study the human motor adaptation to external perturbations/assistance to the ankle [8]–[10], [17], [25]–[28], and to a lesser extent to the knee [13], [19], and the hip joints [29]. To date, these studies have mostly focused on performance augmentation using exoskeletal assistance and how human gait patterns adapt to the external perturbations.

Differing from the design and experimental efforts described previously, we have developed a left and right similar quasi-passive knee exoskeletons that allow us to investigate the performance of the knee joint in interaction with varying passive external impedances (stiffnesses) that we hypothesize will allow users to reduce their muscle forces and joint moments while retaining the overall kinematic and kinetic patterns of the gait. The device implements a spring in parallel with the knee joint in the WA phase of the gait and releases it throughout the rest of the gait cycle, shown in Fig. 2.

We chose to investigate the knee joint because among lower extremity joints, it demonstrates several major functions in walking: supporting the weight of the body, absorbing shocks resulting from heel strikes in the stance phase of the gait, flexing in the swing phase to enable foot clearance and obstacle avoidance, among others [21], [23]. Furthermore, the knee demonstrates the most "spring-like" behavior of the three leg joints during normal walking [21], [23], leading researchers to develop exoskeletons that semipassively implement a spring in parallel with the knee to assist this joint in the stance phase [6], [13].

The spring-like behavior of the knee joint in the stance phase emerges from complicated interaction of the underlying biolog-
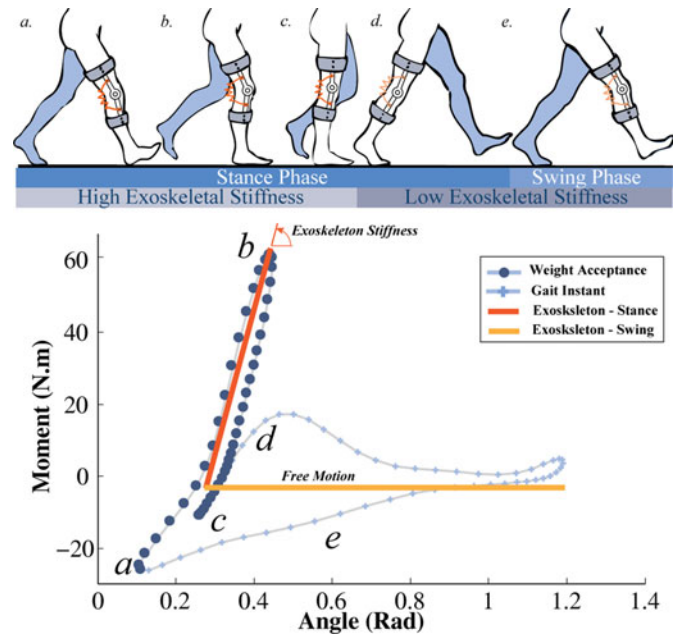

Fig. 2. (Top) Exoskeleton implements a high-stiffness spring in the weight acceptance phase of the gait and a low-stiffness spring throughout the rest of the gait cycle. (Bottom) Exoskeleton implements a spring stiffness equivalent to estimated knee quasi-stiffnesses of the volunteers.

ical mechanisms [23], [30], but can be suitably characterized by the concept of quasi-stiffness, which is the slope of the linear fit to the moment-angle graph of the knee joint in the stance phase, as well as joint excursion in the stance phase [21], [23], [31]. This emergent spring-like behavior is studied here in interaction with externally implemented parallel springs which behave similarly to the knee joint. One should differentiate joint quasi-stiffness from joint stiffness; in that the former refers to the overall moment-angle behavior of a joint in a locomotion task and the latter refers to static/dynamic stiffness of a joint at a certain configuration [22], [23], [30], [32].

We begin the next portion of this paper by describing the mechanical design and control scheme of the devices. We continue with the moment-angle characterization of the exoskeletons and a theoretical model of the devices in interaction with the human limbs. We then describe preliminary experiments on three healthy adults and present intersubject mean and standard deviation (SD) of the angle and moment profiles of the lower extremity joints in the sagittal plane. The preliminary results of this study show that the exoskeletons can apply substantial torques to the knee joint in the WA phase of the gait without notably affecting the kinetic and kinematic profiles of the lower extremity joints, implying motor adaptation by the wearers.

II. EXOSKELETON DESIGN

A. Background and General Approach

A gait cycle is defined as the period between two consecutive heel strikes of the same foot with the ground, and is composed of a stance phase where the foot is on the ground and a swing phase where the foot is off the ground, as schematically shown
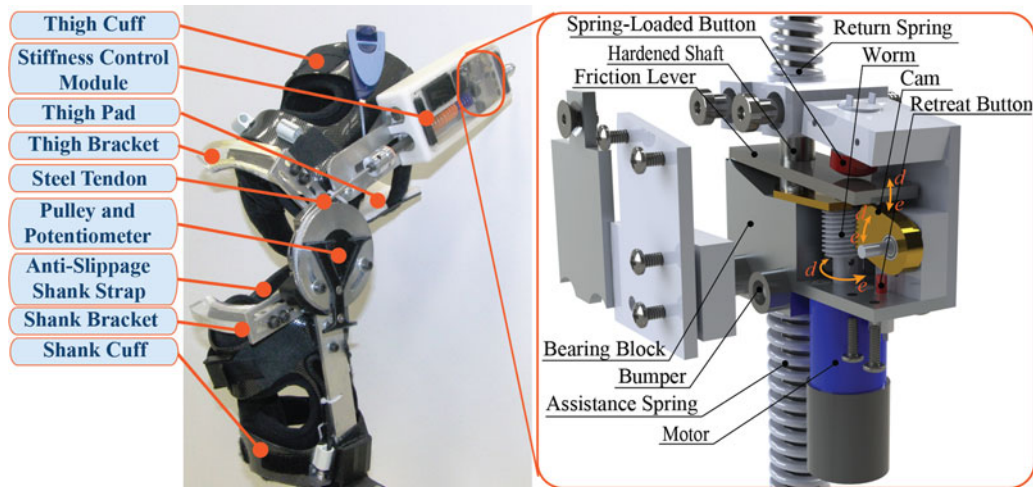
Fig. 3. (Left) Quasi-passive knee exoskeleton is composed of a SCM that is assembled on the thigh segment of the exoskeleton, and a pulley on the shank segment. The shank segment is coupled to the SCM through a steel tendon. (Right) SCM employs a friction-based latching mechanism to engage/disengage an assistance spring. The directions of movement of the motor and worm-gear set for engagement and disengagement are illustrated. Particularly, the motor spins counterclockwise, and the cam and friction lever downward to engage and vice versa to disengage.

in Fig. 2(top). The stance phase comprises a WA (first ∼40%, as depicted in Fig. 2 points a to c) and a terminal stance (∼40–63%, as shown in Fig. 2 points c to d) subphases [21], [23], [33]–[35]. The human knee demonstrates a linear flexion stage (points a to b in Fig. 2) and a linear extension stage (points b to c in Fig. 2) in the WA phase of the gait for normal, level-ground walking [21], [23].

Researchers have recently proposed the concept of quasi-stiffness, as the slope of a linear fit to the moment-angle data of a lower extremity joint in a period of the gait, to approximate the behavior of that joint within that period [31], [32], [36]–[39]. Previous research shows that the knee quasi-stiffnesses in the flexion and extension stages of the WA phase tend to be identical at the preferred gait speed, implying that the knee behaves close to a linear torsional spring at the preferred gait speed [21], [23]. The spring-like moment-angle behavior of the knee joint in the WA phase of walking has led researchers to incorporate springs in the design of exoskeletons to attempt to replace the function of the assisted joints [3], [6], [11], [13], [19].

The spring-like moment-angle behavior of the knee joint does not reveal substantial information about the function of the underlying mechanisms responsible for that behavior and the performance of the human joints in interaction with external stiffnesses [22], [23], [30]. Researchers have explored the adaptation of the human lower limbs in interaction with serial impedances [40], [41]. However, limited effort has been directed toward investigation of the interaction between the human limbs and parallel impedances.

In this study, we intend to investigate the kinetic and kinematic behavior as well as the motor adaptation of the knee joint assisted by external parallel springs in the WA phase of the gait. More specifically, we hypothesize that an exoskeletal torsional spring in parallel with the knee joint can fully/partially replace the spring-type behavior of the knee and unload the corresponding muscles in the WA phase of the gait without large variation in overall gait kinematics and kinetics.

B. Design Overview

The quasi-passive knee exoskeletons can demonstrate two levels of stiffness in parallel with the knee joint using a friction-based latching mechanism shown in Fig. 1 and in detail in Fig. 3. Each of the exoskeletons primarily comprises of a thigh segment including a stiffness control module (SCM) and a thigh cuff, and a shank segment including a pulley, a rotary potentiometer, and a shank cuff, as shown in Fig. 3. The SCM includes a shaft that is attached to the pulley by a steel tendon and can slide upward and downward as a result of knee movement. The SCM includes a return spring that remains engaged at all times and pushes the SCM shaft upward throughout the gait cycle. The return spring has a relatively low stiffness and it primarily returns the shaft to its original position (most proximal) during the knee extension. The left and right exoskeletons were similarly designed and made.

The SCM employs a friction-based latching mechanism to engage and disengage the assistance spring and act on the shaft. A shaft movement due to knee flexion always compresses the return spring, whereas a shaft movement due to flexion only compresses the assistance spring when the latching mechanism has engaged it. As such, the linear stiffness of the SCM acting on the shaft would be the summation of the stiffnesses of the assistance and return springs when the assistance spring is latched, and only the stiffness of the return spring when the assistance spring is unlatched (see Fig. 6 for a schematic representation of this behavior).

The tendon connected to the SCM shaft wraps around a pulley that rotates together with the knee joint and pulls the shaft of the SCM that, in turn, transforms the linear stiffness of the SCM springs to a torsional stiffness around the knee joint. Fig. 3(right) illustrates the design of the exoskeletons latching mechanism that is composed of a friction lever, shaft, bearing block, dc motor, worm-gear, cam, spring-loaded push button, and retreat push button, and additional structural components. We have reported

additional details on the latching mechanism in our previous paper on the design of a compliant stance control orthosis that employs a similar mechanism [3].

The exoskeletons have been implemented on two adjustable knee braces (SPL2 from Fillauer LLC) that can fit on a wide range of subjects with heights of 1.50–1.85 m (as suggested by the manufacturer). To minimize the effect of soft tissues and to help the exoskeletons withstand the anticipated loads, we reinforced the brace by using 1) a bracket that pressed against the quadriceps femoris tendon and was located ∼5 cm superior to the center of the patella, 2) a bracket that pressed against the tibial tuberosity and was located ∼6 cm inferior to the center of the patella, 3) a solid pad that was placed posterior to the thigh and under the strap of the knee brace thigh cuff, and 4) a suspension harness strap that vertically supported the exoskeletons from the shoulder and avoided downward migration of the brace.

C. Friction-Based Latching Mechanism

The latching mechanism employs a motor to manipulate a friction lever to initiate or release a friction-based latch. The latching mechanism includes a worm-gear set that transforms motor rotation to a linear motion at the friction lever. To engage the assistance spring, the motor spins the worm gear counterclockwise to retreat the cam from the friction lever and make ∼2 mm clearance under it, as shown in Fig. 3(right). This movement continues until the cam presses the retreat button that sends a feedback signal to the controller. Upon the retreat of the gear, the spring loaded push button presses the friction lever down and against the shaft to initiate a friction-based latch. The latching grip of the friction lever occurs when the shaft moves downward (as a result of a knee flexion) and the interaction force between the bearing block and the friction lever induces higher normal forces between the friction lever and the shaft. As such, the bearing block moves along with the shaft and compresses the assistance spring. An upward movement of the shaft (mainly caused by the return spring during the knee extension) relaxes the friction forces on the friction lever at the contact points and releases the latching grip when the assistance spring is totally unloaded. Therefore, the latch only initiates in the flexion direction and it is maintained during extension only if the assistance spring is engaged and loaded.

To disengage the assistance spring, the motor rotates the worm clockwise to move the cam upward and toward the friction lever. The cam lifts the friction lever and releases the latching grip. The upward movement of the lever terminates when the spring-loaded push button is pressed and a feedback signal is sent to the controller to stop the motor. Upon the disengagement of the lever, the shaft freely slides inside the bearing block and friction lever without any force being transferred to the assistance spring. Accordingly, a downward force (e.g., resulting from knee flexion in the swing phase) on the shaft only compresses the return spring. To allow free rotation in the swing phase, we chose a highly compliant return spring (5 Nm/rad), which primarily returns the shaft to its most proximal location after the swing phase without applying a considerable moment
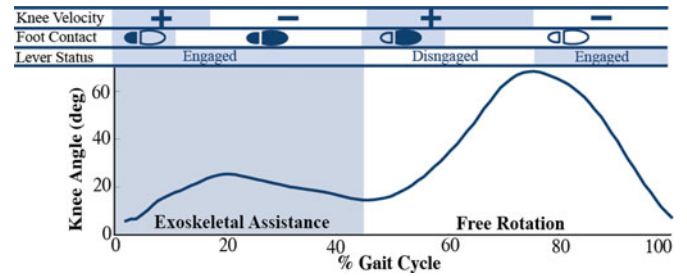

Fig. 4. (Top) The statuses of the knee angular velocity (+ for flexion and—for extension), foot contact with the ground (heel and toe sensors of the instrumented shoe insole), and friction lever in a gait cycle. (Bottom) Knee angle profile of a volunteer walking at 1.25 m/s. The exoskeleton assists the knee in the weight acceptance phase of the gait and allows free motion in the rest. The shades roughly show the timing of state changes.
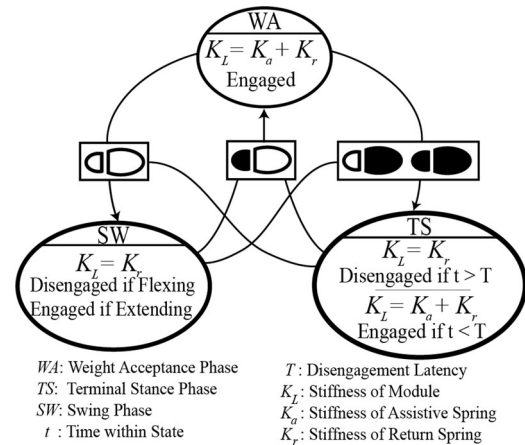

Fig. 5. Diagram of the finite state machine that the exoskeleton controller uses to engage/disengage the assistance spring. The states include weight acceptance (WA), terminal stance (TS), and swing (SW) and are identified using a foot sensor. The diagram also indicates the engagement status of the friction lever and stiffness of the module.

to the knee. A more detailed explanation of the friction-based latching mechanism can be found elsewhere [3].

D. Control Scheme

The control unit implements a finite-state machine for the engagement of the assistance spring during walking. The assistance spring has to be engaged during the WA phase of the gait and allow free rotation throughout the rest of the gait, as schematically shown in Fig. 2(top). The controller identifies the states using an instrumented shoe insole that indicates the heel and toe contacts with the ground. Fig. 4(top) shows the status of the heel and toe sensors of the insole, the sign of the knee velocity (positive for flexion) measured by a rotary potentiometer that is embedded in the exoskeleton pulleys, as well as the status of the friction lever within a gait cycle. Fig. 4(bottom) shows the knee angle profile for a volunteer walking at 1.25 m.s^{-1} on a level ground and the period where the assistance spring is intended to be engaged and loaded. Fig. 5 describes the finite-state machine that consists of the following states.

1) *Weight Acceptance (WA):* The heel sensor is on and toe sensor is off. The controller engages the assistance spring.
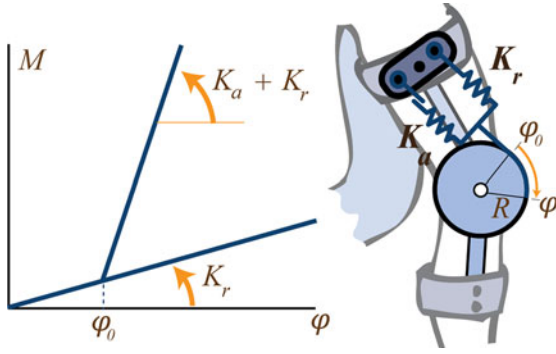
Fig. 6. (Left) The moment-angle characterization of the exoskeleton. K_a is the stiffness of the assistance spring, K_r is the stiffness of the return spring, φ_r is the angle of engagement, M is the exoskeleton moment, φ is the exoskeleton angle, and φ_0 is the angle at which the assistance spring is engaged. (Right) Schematic model of the exoskeleton. A clutch mechanism engages/disengages the assistance spring.
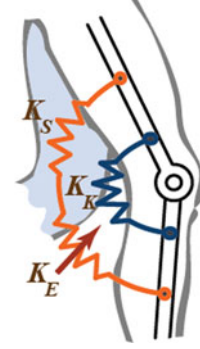

Fig. 7. Schematic model of the knee complex comprising the knee equivalent spring, exoskeleton spring, and the compliance of the biological soft tissues of the leg and exoskeleton cuffs. The assistance condition includes modulation of K_E, whereas we primarily intend to investigate the effect of external parallel spring on the spring-type behavior of the knee joint.

2) *Terminal Stance (TS):* The toe sensor is on and heel sensor is off, or both toe sensor and heel sensor are on. The controller disengages the assistance spring after a period of time ($T = 60$ ms, measured on a knee simulator as explained later in this text) dictated by the latching mechanism latency plus an adjusted period of time that nearly coincides with the end of the weight acceptance phase.

3) *Swing (SW):* The toe and heel sensors are off. The controller monitors the knee velocity direction during the swing phase to identify whether the knee is flexing or extending. The controller unlatches the friction lever during the flexion period of the swing phase and latches it during the extension period, as a precautionary measure against the latching mechanism latency. Because engagement of the assistance spring can only initiate in the flexion direction (positive sign of knee velocity, see also Fig. 4), latching of the friction lever in the extension period of the swing phase does not result in engagement and loading of the assistance spring and impeding knee joint motion.

We developed two finite-state machines, one for each exoskeleton, on a microcontroller MPC5534 from Freescale Semiconductor Company (MPC5534EVBE). The controller measured the knee angle using a rotary potentiometer that is integrated inside the exoskeletons pulleys and the knee velocity by differentiating the potentiometer signal. We used an instrumented shoe insole from B & L Engineering Co., a Faulhaber 2224 dc motor (4.05 W), a rotary potentiometers from Vishay Co. model 357 for each exoskeleton, a dual H-Bridge circuit from Solarobotics Company, and a battery pack with a capacity of 2500 mAh. The controller transfers the signal from the spring-loaded push button to identify if the friction lever is disengaged, and the signal from the retreat push button to identify if the friction lever is engaged. We used a serial-to-Bluetooth adapter (Wireless RS232, Willies Computer Software Co.) to wirelessly transfer the data to a host LabView module implemented on a computer for data collection. The data include the left and right exoskeletons joint angles and status of engagement of the lever based on which we calculated the exoskeleton moments.

E. Moment-Angle Characterization

In the previous section, we explained that the linear stiffness of the exoskeleton (K_L) transforms to a rotational stiffness around the knee joint (K_E) through a tendon that connects the SCM shaft to the exoskeleton pulley. Fig. 6(right) schematically shows the function of the exoskeleton. In our previous work, we showed K_L and K_E are related as [3]:

$$K_E = K_L \cdot R^2 \qquad (1)$$

where $R = 5$ cm is the radius of the exoskeleton pulleys, K_L is the stiffness of the return spring when the friction lever is disengaged, and the sum of the stiffness of the assistance spring (K_a) and return spring (K_r) when the assistance spring is engaged:

$$K_L = \begin{cases} K_r + K_a & \text{engaged} \\ K_r & \text{disengaged.} \end{cases} \qquad (2)$$

Combining (1) and (2), the exoskeletal rotational stiffness can be expressed as

$$K_E = \begin{cases} (K_r + K_a) \cdot R^2 & \text{engaged} \\ K_r \cdot R^2 & \text{disengaged.} \end{cases} \qquad (3)$$

Therefore, the exoskeleton assistive moment is related to the knee joint angle (φ) as follows:

$$M_E = \begin{cases} K_r \cdot R^2 \cdot \varphi + K_a \cdot R^2 \cdot (\varphi - \varphi_o) & \text{engaged} \\ K_r \cdot R^2 \cdot \varphi & \text{disengaged.} \end{cases} \qquad (4)$$

Here, φ is the knee angle and φ_o is the angle at which the assistance spring is engaged. Fig. 6(left) schematically shows the moment-angle performance of the exoskeleton. The exoskeleton controller records φ and φ_o from the potentiometer, and status of the spring engagement for both left and right exoskeletons from the push buttons incorporated in the SCM, and wirelessly transfers them to a host computer. We combined the controller data with the exoskeleton spring stiffnesses and obtained the exoskeleton moments.

The exoskeletons compliantly interface with the human limbs as a result of compliance in the biological soft tissues and exoskeleton cuffs and attachments. We approximate this by an

additional spring between the assistance spring and the thigh. Fig. 7 schematically shows the configuration of the three springs of the knee complex that represent the knee joint, exoskeleton, and soft tissue behavior in the *weight acceptance phase* of the gait. This theoretical model suggests

$$K_C = K_K + K_X \qquad (5)$$

where K_C is the quasi-stiffness of the knee complex, K_K is the quasi-stiffness of the knee joint, and K_X is the external parallel stiffness that is equal to

$$K_X = \frac{K_E K_S}{K_S + K_E} \qquad (6)$$

where K_E is the exoskeleton stiffness and K_S is the interface stiffness. In fact, K_X is the externally applied parallel stiffness that is being perceived by the anatomical knee joint. We also define θ_C as the excursion of the knee complex, θ_K the excursion of the knee joint, θ_E the excursion of the exoskeleton, and θ_S the excursion of the interface in the weight acceptance phase. One should note that θ_E is the range of changes of φ in the weight acceptance phase.

III. MECHANICAL AND FUNCTIONAL EVALUATION

A. Mechanical Evaluation

We tested the reliability of the exoskeleton and measured the latency of the SCM using a knee joint simulator prior to the human trials, as schematically shown in Fig. 8(top). In testing the reliability of the exoskeleton we conducted, extensive testing to ensure that the exoskeleton can withstand the dynamic loads it would encounter in walking, and to ensure that the exoskeleton can undergo the number of gait cycles that we expect during the experiments on human volunteers.

The knee simulator primarily consists of a large four-bar linkage driven by a three-phase servomotor and servo controller (SGMAV-10A3A61 from Yaskawa and SGDV120AE from Omron Companies) [42]. The servomotor emulates the kinematic profile of the knee joint and sends a digital signal to the SCM to engage the support spring during the simulated stance phase and disengage during the rest of the gait, as shown in Fig. 8(bottom). The simulator records the actual instances of engagement/disengagement using the feedback signals from the push buttons embedded in the SCM. We estimate the engagement/disengagement latency by measuring the time period between the command and feedback signals. The latencies could alternatively be approximated by the properties of the dc motor and worm-gear set of the engagement mechanism; a method that was ignored because friction and other imperfection in the mechanism could not be characterized. We fabricated a prototype of the SCM and tested it on the knee joint simulator as schematically shown in Fig. 8(top).

The prototype successfully underwent $\sim$30 000 gait cycles (with maximum moment of 60 Nm/rad) on the knee simulator without any failure in the mechanical components and engagement occurrence. The average latencies for both engagement and disengagement were also measured using the test machine and were found to be $T = \sim$60 ms. We explained earlier that the ex-
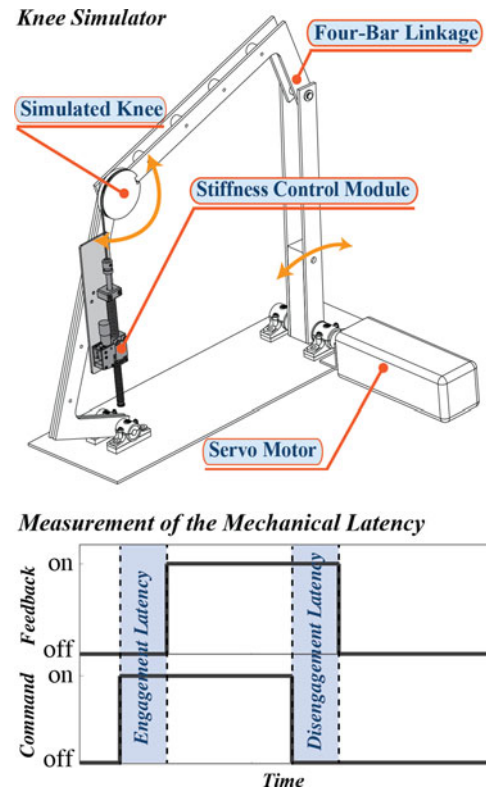

Fig. 8. (Top) SCM mechanically tested on a knee simulator. The simulator is primarily a four-bar linkage mechanism driven by a servo motor. The SCM is mounted on the simulator and undergoes numerous working cycles to endure the reliability and functionality of the module and measure the mechanical latency of engagement/disengagement. (Bottom) The simulator controller sends an engagement command signal to the compliance control module and receives the feedback from the push buttons embedded in the module. The time differences between these signals indicate the mechanism engagement/disengagement latency.

oskeleton transferred the engagement signal to a host computer to calculate the exoskeleton moment profiles. The engagement signal was extended by 60 ms to capture the effect of the disengagement mechanism latency. The disengagement latency (T) was also used in the design of the state machine of Fig. 5. One should note that the engagement latency was not used because the exoskeletons engage the spring in the extension period of the swing phase and prior to the heel contact with the ground.

The mechanical function of the exoskeletons was also monitored using a high-speed camera to visually inspect the mechanism function in additional detail. The video analysis confirmed that the engagement mechanism functioned as desired throughout the experiments.

B. Experimental Protocol and Instrumentation

The testing protocol included two experimental conditions of treadmill walking, which are described as follows.
1) Control Condition (*CTRL*): included the volunteers walking on a treadmill without wearing the exoskeletons.
2) Assistance Condition (*ASSIST*): included the volunteers walking with the exoskeletons with assistance spring stiffness equivalent to the quasi-stiffness of the anatomical knee, which requires knowledge of the knee

Volunteer	Gender	Age	Height (m)	Weight (kg)	Exoskeleton Stiffness ($^{Nm}/_{rad}$)
1	M	26	1.83	68.0	240
2	M	23	1.68	71.0	240
3	M	29	1.77	66.7	240
	Mean	**26**	**1.76**	**68.6**	**240**
	SD	**3**	**0.75**	**2.2**	**0**

quasi-stiffness in walking on the level ground. This information was not known prior to the experiments; therefore, we used the statistical models we developed and tested in a previous study to estimate each volunteer's knee quasi-stiffness in the weight acceptance phase of the gait according to the following expression [23]:

$$K_E = 5.21\, \text{W}\sqrt{H^3} - 7.50\, \text{W}\sqrt{H} - 5.83\, \text{WH} + 11.64\, \text{W} - 6 \tag{7}$$

where W (kg) is weight and H (m) is height of the volunteer. We chose a spring stiffness that is commercially available and with stiffness close to the estimated values, as reported in Table I. This model was shown to be accurate with a 9% error of estimation and was established for volunteers with a wide range of weight (from 67.7 to 94.0 kg) and height (from 1.43 to 1.86 m) [23].

The study protocol was approved by Yale University Institutional Review Board, Human Use Review Committee of United States Army Research Institute of Environmental Medicine, Army Human Research Protections Office, and Battelle Institutional Review Board. We recruited three healthy adult volunteers from the US Army Soldiers assigned to Headquarters, Research, and Development Detachment of Natick Soldier System Center. We ensured that the volunteer heights and weights are within the range recommended by the manufacturer (1.50 to 1.85 m for the height and below 130 kg for the weight). Table I lists the demographics of the volunteers, including the means and standard deviations of weight, height, gait speed, and age, as well as the stiffness of the assistance spring of the exoskeleton for each volunteer.

The experimental protocol included a total of three visits including two initial orientation sessions and the actual experimental visit as last. The three visits took place in one week with one to two day(s) in between to provide rest and prevent any fatigue effect that could affect the results. Volunteers' weight and height were measured on the first visit to also size the assistance spring stiffness for the assistance conditions.

Orientation Sessions: Two orientation sessions prior the main experiment were included to allow the volunteers to familiarize to walking with the exoskeletons. The participants wore Army Physical Fitness Uniforms including shorts, t-shirts, socks, and their own athletic shoes. To become familiar with walking on a treadmill, the participants walked on the treadmill for 3 min at 4.83 km/h, after which they were given a 3–5 min rest break. We then instructed each participant to walk on the treadmill and slowly increased the speed from the zero state up to the self-selected comfortable pace. We used this pace as the preferred gait speed throughout the experiments.

We fitted the exoskeletons on the volunteers while they were sitting and ensured that the left and right exoskeleton joints and knee joints were aligned. The suspension harness straps were also put on the volunteer and fastened on the controller belt, which was strapped around the shoulders. Finally, we adjusted the tension of suspension straps to prevent vertical migration of the exoskeletons as the volunteer slowly stood up. On the first orientation visit, the volunteers were asked to walk overground wearing the exoskeletons for the assistance condition but not for the control condition. For each condition, they walked overground for about 640 m at their own pace, covering a distance approximately equivalent to the distance covered in 8 mins of treadmill walking. A 5-min seated rest break was given to the volunteers before they walked on the treadmill in the same condition for 8 min at their preferred gait speed. The order of the conditions for the first session was kept the same and not randomized across volunteers. The second orientation day included trials of 10-min treadmill walking only and the order of the two experimental conditions were randomized for each volunteer. The order of the conditions was the same as the one followed during the data collection session. To summarize, volunteers walked a total 18 min on the treadmill and 10 min overground for each of the two conditions during the first two orientation sessions.

Data Collection Sessions: The participants wore tight t-shirts, spandex performance shorts, and their own athletic shoes. Reflective markers were placed on body landmarks according to convention previously described in [43], with the slight difference in that we placed four-marker clusters on the shank and the thigh such that the exoskeleton cuffs could fit on the limbs without blocking their visibility from the cameras. Additionally, a four-marker cluster was placed on the chest to track the trunk and pelvis as a single segment. The same randomized order of the experimental condition used in the second orientation session was also used in this session with 8–10 min trials of treadmill walking. Within each trial, a 30-s long data recording was taken after 4 min from the start of the trial.

Data collection took place at Center for Military Biomechanics Research at the US Army Natick Soldier Research, Development and Engineering Center, Natick, MA, USA. The experimental conditions included walking on a custom-made force plate treadmill (fabricated by AMTI, Watertown, MA, USA). The treadmill comprises two synchronized treadmill belts positioned side by side, each on a separate force platform with a gap smaller than 1 cm. We used a ten camera motion capture system (Qualysis, Gothenberg, Sweden) and Qualisys Track Manager Software to track lower limb markers and calculate kinematic profiles. The exoskeletons simultaneously transferred data of right and left exoskeleton joint angles, heel and toe sensors status, and feedback signal from the spring-loaded and retreat push buttons as indicators of the status of the friction lever engagement to a host computer. The exoskeleton also sent a synchronization signal to the Qualisys camera system that allowed us to synchronize the data from the two data acquisition systems.

TABLE II
MASS PROPERTIES OF THE EXOSKELETON

Side	Segment	Weight (kg)	$I_{xx} (kg.m^2)$	$I_{yy} (kg.m^2)$	$I_{zz} (kg.m^2)$
Right	Thigh	1.68	0.02370	0.02312	0.00211
	Shank	0.77	0.00217	0.00249	0.00122
Left	Thigh	1.81	0.02370	0.02312	0.00211
	Shank	0.82	0.00217	0.00249	0.00122

Left Exoskeleton Weight = 2.63 kg.   Right Exoskeleton Weight = 2.45 kg.
Controller Unit Weight = 2.4 kg.   Total Weight = 7.48 kg.

C. Kinematic and Kinetic Profiles

We used visual 3-D software (C-Motion, Gaithersburg, MD, USA) to calculate the lower extremity joints kinematic and kinetic profiles. To obtain the moment profiles for the conditions that included a device, we first calculated the mass and moment of inertia and the center of mass of the exoskeleton thigh and shank segments in SolidWorks, as listed in Table II. We accordingly updated the mass, center of mass, and moment of inertia of the shank, thigh, and trunk segments and conducted inverse dynamics analysis to obtain the moment and power profiles in the sagittal plane. To approximate the moment of the knee joint in the sagittal plane, we subtracted the synchronized moment of the exoskeleton from the moment of the complex assuming that the axis of exoskeleton joint is perfectly aligned with the knee joint axis.

D. Profile Comparison Measures

We identified the gait cycles by the right heel strikes. We found that at least four consecutive gait cycles (four left strides and four right strides similar to the approach of others [4]) for each trial had proper force plate signals. Therefore, we obtained the intrasubject average angle, moment, power, and force profiles of four consecutive cycles for each trial to be consistent among the trials. We normalized the intrasubject mean angle profiles with respect to the standing configuration and moment profile by dividing by the body mass. The intersubject mean and SD profiles were obtained from the intrasubject mean profiles. The coefficient of variability (CV described elsewhere [34]) was also calculated for each profile using the mean and SD profiles. As suggested by other researchers [17], we compared the kinematic and kinetic profiles of the CTRL and ASSIST conditions using linear regression between the intersubject mean profiles under these two conditions. The R^2 value of the regression indicates the degree of similarity of the patterns, while the slope refers to the scaling factor. For example, a profile identical to the control profile would have an R^2 and a scale of 1, whereas a down scaled profile (i.e., smaller range of values) with identical pattern would have $R^2 = 1$ and slope <1. One should note that the scale is not very meaningful when R^2 is relatively low.

E. Moment-Angle Analysis

As mentioned earlier, the knee joint moment-angle data were obtained by subtracting the exoskeleton moment from the overall knee complex data obtained from the inverse dynamic analysis. To obtain K_C and K_K, linear polynomials were respectively regressed on the moment-angle data of the knee complex and knee joint in the weight acceptance phase of the gait (points a

to c in Fig. 2). The slopes of the corresponding linear fits represent K_C and K_K, and the coefficient of determination (R^2) indicates the goodness of the fit representative of the linearity of the behavior of the knee complex and knee joint in the weight acceptance phase. We subtracted the minimum angle from maximum angle of the knee complex in the weight acceptance phase to calculate the knee complex excursion (θ_C) and similarly for the knee joint excursion (θ_K). We similarly calculated θ_E by subtracting the minimum angle from the maximum angle of the exoskeleton in the weight acceptance phase and θ_S by subtracting θ_E from θ_C.

IV. RESULTS

A. Kinematic and Kinetic Profiles

Fig. 9 shows the joint angle and moment profiles for CTRL condition (dashed gray) and ASSIST condition (solid black). The first row corresponds to the ankle joint, second row the knee complex, and third row the hip joint in the graphs of each parameter. The left and right columns correspond to the left and right sides, respectively. The thick solid lines indicate the intersubject mean profiles and the thin lines ± 1 SD boundaries. The gait cycles were identified by the right heel strikes. The legends of each graph indicate the CV of each profile in parentheses followed by the R^2/Scale. The values of R^2/Scale for the ASSIST condition are with respect to CTRL condition.

The intersubject average angle and moment profiles shown in Fig. 9 indicate that the exoskeleton assistance does not appear to have a considerable effect on the pattern of angle and moment profiles of all the lower extremity joints in the sagittal plane. In particular, the average angle profiles between the CTRL and ASSIST conditions appear to be very close or overlapping in the stance phase of the gait cycle where the assistance spring is engaged, while more separation between the profiles of the two conditions is noticeable during the swing phase of the gait cycle. This behavior appears to hold true across all joint profiles in the swing phase and may likely be attributable to the mass of the exoskeletons (2.63 kg for the left and 2.45 kg for the right exoskeleton). To quantify the previous qualitative observations, Fig. 9 reports the values of R^2/Scale for ASSIST condition with respect to the CTRL condition. The high R^2 values reported in Fig. 9 support the observation that the external assistance does not have a considerable effect on the pattern of angle and moment profiles of the lower extremity joints in the sagittal plane. We can observe a slight downscale in the knee and ankle angle profiles, and both upscale and downscale in hip angle profile in the sagittal plane. All joint moment profiles in the sagittal plane exhibit an upscale in the range of values, except for the right knee which shows a downscale.

Fig. 10(top) shows the intersubject mean angle profiles for the knee joint (black) and exoskeleton (dashed gray). Here we observe that the exoskeleton flexion in the weight acceptance phase (as distinguished by light gray dashed stripes) is considerably smaller than the knee joint, implying that the interface between the exoskeleton and the leg undesirably compresses under the effect of the interface force between the exoskeleton and the limbs. Fig. 10(middle) shows the mean intersubject moment profiles for the knee joint (black), exoskeleton (dashed
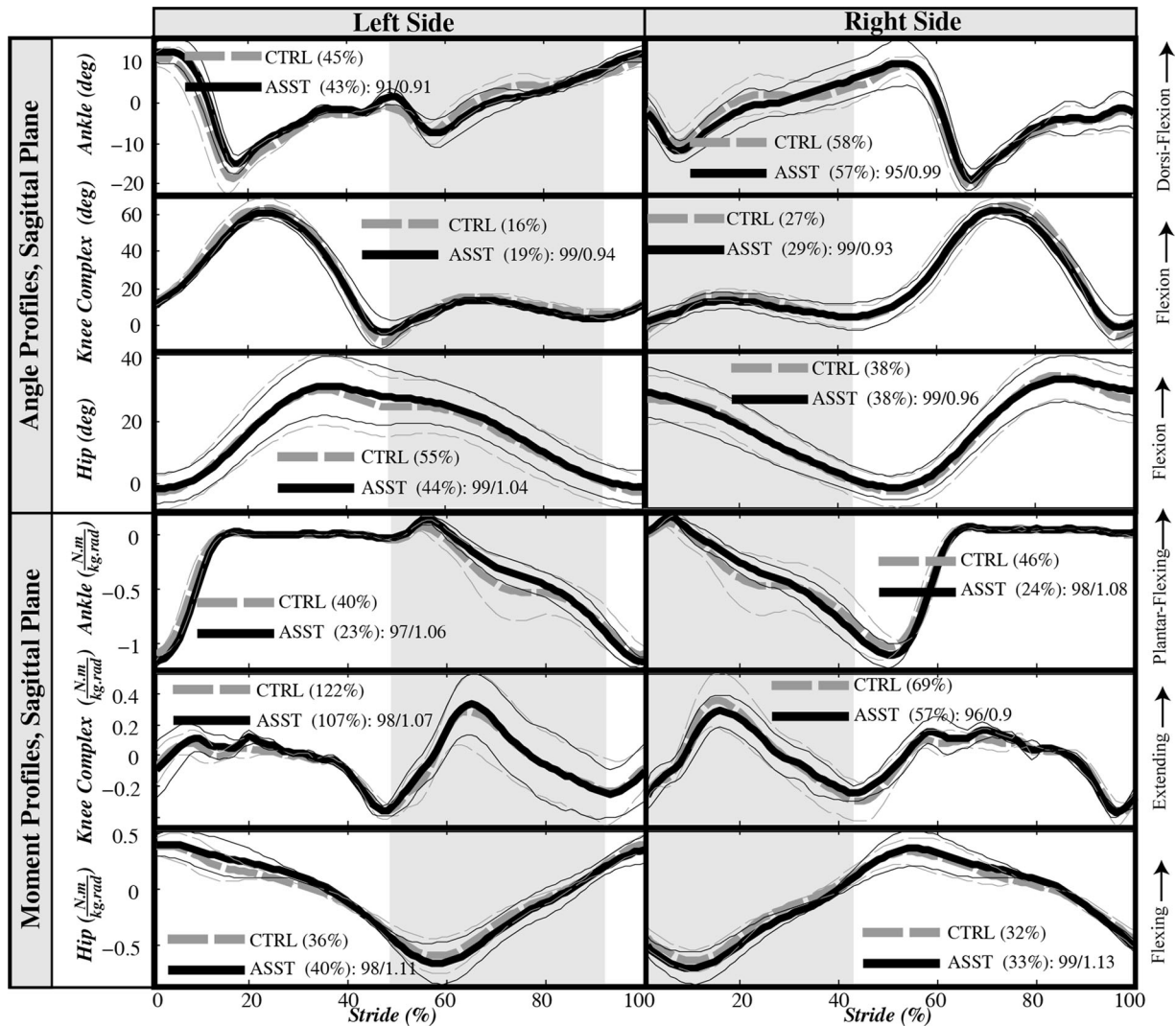
Fig. 9.   Inter-subject angle and moment mean and ± 1 SD profiles of lower extremity joints in the sagittal plane. The left and right columns correspond to the left and right joints, respectively. The first, second, and third rows, respectively, correspond to the ankle joint, knee complex of anatomical knee joint and exoskeleton, and hip joint in the top and bottom sets of graphs. The dashed gray and solid black colors respectively correspond to CTRL and ASSIST conditions. The legends include the coefficient of variability in the parentheses that are followed by the R^2/Scale of the regression between the ASSIST and CTRL mean profiles, where a Scale >1 means that ASSIST profile is scaled up (i.e., greater range of values) with respect to the CTRL condition. The assistance period is indicated by a shaded area.

gray), and knee joint complex (light dashed gray). We observe that both left and right exoskeletons have been able to engage the assistance spring and apply substantial moments to the knee joint in the weight acceptance phase, and that the knee angle profile is largely maintained in the presence of this loading. Fig. 10(bottom) shows the mean intersubject power profiles for the knee joint (black), exoskeleton (dashed gray), and knee joint complex (light dashed gray). The graphs show that the right exoskeleton resulted in higher peak power values for the right knee joint and smaller peak power values for the left knee joint in the weight acceptance phase.

B. Effective Parallel Stiffness

Fig. 11 shows a sample moment-angle graph for the first subject. The graph includes the moment-angle graph of the knee complex, knee joint, and exoskeleton for ASSIST condition,

and the moment-angle graph of the knee joint for CTRL condition. The linear fits associated with the quasi-stiffness values are also shown in this figure. The first to third rows of Fig. 12, respectively, show the quasi-stiffness, excursion, and R^2 values of the knee complex for the CTRL and ASSIST conditions. The left and right columns respectively indicate the left and right knee complexes. The first row illustrates the intersubject mean knee complex and knee joint quasi-stiffnesses and exoskeleton stiffness for the left and right side. We observe that $\bar{K}_X = 0.78$ Nm/kg.rad $(\text{SD}_{\bar{K}_X} = 0.39$ Nm/kg.rad$)$ for the left exoskeleton and $\bar{K}_X = 1.72$ Nm/kg.rad $(\text{SD}_{\bar{K}_X} = 0.32$ Nm/kg.rad$)$ for the right exoskeleton. Considering the series arrangement of the exoskeleton spring and interface compliance, the effect of the interface stiffness on the performance of the left exoskeleton is substantially higher than the right exoskeleton. In fact, we observe that the excursion of the interface between the left exoskeleton and the leg $(\bar{\theta}_S = 8.0°$
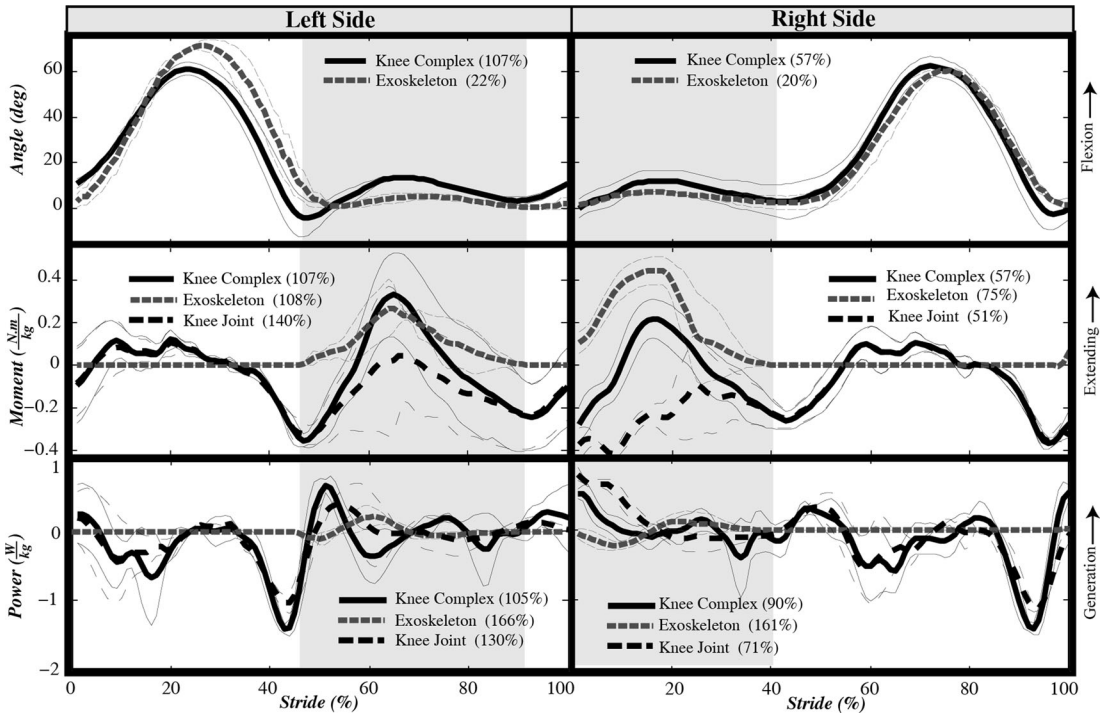
Fig. 10. (Top) Inter-subject angle mean and ±1 SD profiles of the knee complex and exoskeleton in the sagittal plane. (Middle) Inter-subject moment mean and ±1 SD profiles of the knee complex, anatomical knee joint, and exoskeleton in the sagittal plane. The knee joint moment profile is obtained by subtracting the exoskeleton moment from the knee complex moment. (Bottom) Inter-subject power mean and ±1 SD profiles of the knee complex and exoskeleton in the sagittal plane. The solid black and dashed gray colors respectively indicate the knee and exoskeleton profiles. The black dashed lines show the profiles of the knee joint. The exoskeleton provides assistance in the weight acceptance phase, which is illustrated by the shaded area on each graph.
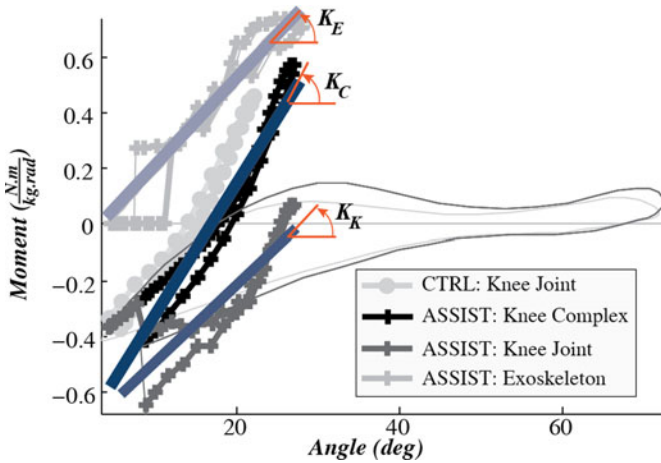

Fig. 11. Sample moment-angle graph for the first subject. Two gait cycles are included: 1. Control condition (light gray circles), 2. Assistance condition (shown by crosses) that includes the graph of the knee complex, knee joint, and exoskeleton. The graph also includes the quasi-stiffness of the knee complex (K_C) and knee joint (K_K) in the weight acceptance phase as well as the stiffness of the exoskeleton (K_E).
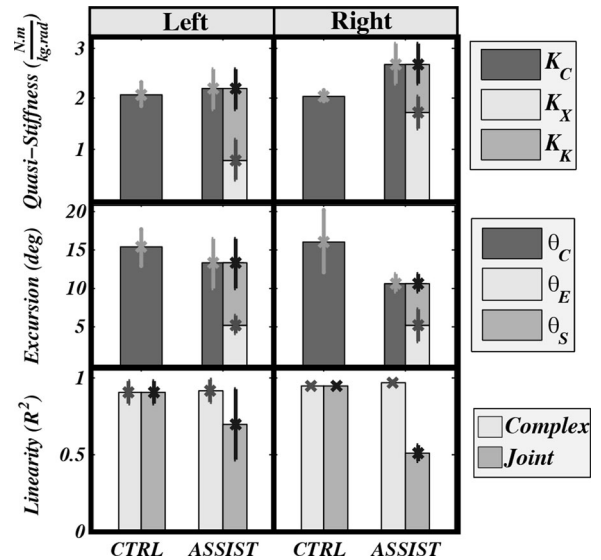

Fig. 12. Inter-subject moment-angle analysis of the knee complex, joint, and exoskeleton in the sagittal plane. The left and right columns correspond to the left and right knee, respectively. The first to third rows are respectively the quasi-stiffness, excursion, and R^2 values in the weight acceptance phase. Note that K_c is the knee complex and K_K is the knee joint quasi-stiffness, and K_X is the external stiffness in parallel to the knee joint, which is a series combination of the exoskeleton stiffness (K_E) and soft interface stiffness (K_S).

and $SD_{\bar{\theta}_S} = 2.2°$) is substantially higher than that of the right interface tissues ($\bar{\theta}_S = 5.5°$ and $SD_{\bar{\theta}_S} = 1.7°$), as shown in the second row of the figure. Table III lists the values of the interface rotational stiffnesses for the left and right side indicating that the stiffness of the left side ($\bar{K}_S = 81$ Nm/rad and $SD_{\bar{K}_S} = 12$ Nm/rad) is substantially smaller than that of the right side ($\bar{K}_S = 304$ Nm/rad and $SD_{\bar{K}_S} = 102$ Nm/rad). Ta-

ble III also includes the exoskeleton stiffness for comparison. Considering the consistency of the difference among all the subjects, we can attribute this behavior to structural differences in the exoskeleton cuffs and attachments.

TABLE III
INTRASUBJECT MEAN STIFFNESS OF COMPLIANT INTERFACE BETWEEN EXOSKELETON AND LIMBS

Volunteer	Left Interface Stiffness ($^{Nm}/_{rad}$)	Right Interface Stiffness ($^{Nm}/_{rad}$)	Exoskeleton Stiffness ($^{Nm}/_{rad}$)
1	95	238	240
2	76	422	240
3	73	245	240
Mean	**81**	**302**	**240**
SD	**12**	**104**	**0**

The R^2 values of the third row of the figure indicate that the overall moment-angle behavior of the knee complex remains relatively linear, whereas the knee joint behavior becomes less linear under the effect of exoskeleton assistance. This finding may imply that the human prefers to exhibit an overall linear behavior in the knee complex similar to what the human knee joint exhibits in normal walking on level grounds [21], [23].

V. CONCLUSION AND FUTURE WORK

In this paper, we described a quasi-passive knee exoskeleton that implements a spring with a desired stiffness in parallel with the knee joint in the weight acceptance phase of the gait cycle. We conducted a series of preliminary experiments involving human subjects and found that the knee joint demonstrated a considerable level of motor adaptation to retain relatively invariant kinematic and kinetic profiles; a finding that coincides with the observations of other researchers for the ankle joint [17]. We also found that the patterns of kinetic and kinematic profiles of the hip joint, knee complex (i.e., complex of knee and exoskeleton), and ankle joint in the sagittal plane remained mostly invariant under the effect of the exoskeleton assistance. We also observed that for the three volunteers the exoskeletons was able to engage the assistance spring during the desired period of the gait, providing substantial assistive moments to the knee joint in the weight acceptance phase of the gait.

The reported experiments included one assistance condition with the assistance spring stiffness identical to the estimated quasi-stiffness of the knee joint in normal walking. The experiments also involved a control condition in which the volunteers walked without any device. We found that the exoskeletal assistance only slightly suppresses angle profiles of the joints in the sagittal plane; except, the left hip joint that shows a slight upscale in the range of values. We found that the exoskeleton function and mass resulted in slightly greater moment values in the sagittal plane; except the right knee complex that shows a downscaled profile. We also observed that the interface between the exoskeleton and the leg (comprising of the biological soft tissues of the thigh and shank and the compliant components of the exoskeleton) can excurse more than the exoskeleton joint and dominate the performance of the exoskeleton, negating or obscuring the effect of exoskeletal assistance, depending on the relative stiffnesses of the device and interface. In fact, the moment-angle analysis of the knee complex revealed that the right exoskeleton was able to apply parallel stiffnesses (K_X) comparable to the mean quasi-stiffness of the knee in the con-

trol condition, whereas the left exoskeleton was only able to provide parallel stiffness (K_X) of ~33% of the mean quasi-stiffness of the knee in the control condition, implying that the performance of the left exoskeleton was substantially obscured by the interface compliance. The moment-angle analysis also showed that, although the performance of the knee joint becomes less linear under the exoskeletal assistance, the overall performance of the knee complex tends to remain linear. This suggests that there is a preference for the linear performance of the knee joint in the weight acceptance phase of the gait, which could be attributed to higher rate of energy recovery in this phase [21], [23].

The current study necessitated several assumptions, which should be considered in the interpretation of the results. The reflective markers of the study were mounted on the skin of the volunteer; hence, the kinematic profiles of the knee complex and anatomical joint are assumed to be identical. Additionally, we utilized a suspension harnesses between the exoskeleton and shoulders to minimize vertical migration of the exoskeleton between gait cycles. While the tension on the suspension was only present when the leg was straight, this may have affected the kinetic and kinematic behavior of the joints. Moreover, we calculated the exoskeletons moments by (4). Alternatively, a load cell in the exoskeleton would have allowed for a more direct measurement of the exoskeleton moment, but would have substantially increased the complexity and mass of the device (including the necessary electronics hardware).

To carry out the inverse dynamics analysis, we made several assumptions. We considered the knee joint and exoskeleton as one single joint. Despite the independence of the inverse dynamics analysis of the morphology of the joints, this assumption can have nuisance effects on the joint center estimations and the calculations of the kinetic profiles. We also obtained the exoskeleton moment of inertia and center of mass from a computer-aided design model of the exoskeleton. Therefore, we have ignored the effect of small movements of the exoskeleton with respect to limbs and slight differences between the actual device and the computer models. Our estimation of the knee joint quasi-stiffness using the models we developed in our previous work could impose additional confined effects on the intersubject means and SD calculations [3], [23].

The findings of this research can give insight to the design of exoskeleton for the lower extremity joints (especially the knee joint).

1) We found that replication of the behavior of the knee joint in the stance phase with an external device can provide substantial assistance to this joint and may be a viable assistance strategy for knee exoskeletal devices.

2) The compliance of the biological soft tissues of the leg and the exoskeleton cuffs might neutralize the assistance of an exoskeleton unless it is explicitly accounted for. This is especially true for exoskeletons attached to the thighs, due to the large amount of soft tissue located in those segments. Therefore, the design of exoskeletons should minimize the effect of the soft tissues with additional considerations such as larger pads and more carefully chosen strap locations.

The moment profiles of Fig. 10 indicate that the exoskeleton and knee joint moments had opposite directions in certain periods of the stance phase (at the onset and end of the weight acceptance phase), suggesting that the exoskeleton could impede the knee joint movement in those periods. We also see that the peak power values for the right knee joint increased in the weight acceptance phase whereas that of the left knee joint decreased. Current study includes only three volunteers, which makes the profiles very sensitive to differences between individuals. In future, we intend to study this aspect of the performance of the exoskeleton by examining EMG activities of the underlying muscles across a larger group of volunteers to identify what/if muscles are being assisted or additionally loaded.

All together, the findings of this research suggest that the quasi-passive knee exoskeleton developed here can be used to study the behavior of the knee joint in interaction with external impedances. The preliminary results of this study also suggest that the quasi-passive assistance of the exoskeleton can help reduce the moment profile of the human knee joint in the sagittal plane. It should be pointed out, however, that the participants that were recruited were of similar age, height, and weight and the same exoskeleton stiffness setting was applied to all participants, thus experimental results ought to be conservatively interpreted. However, current results are intended to only show that the exoskeleton functioned as intended and to provide preliminary evidence that the lower extremities demonstrated a level of adaptation. Future research will recruit a larger sample size of participants and investigate the EMG activities of the muscles adjacent to the knee joint and analyze the performance of muscles in interaction with the exoskeletons, as well as investigating the effect of the exoskeleton on the metabolic cost of movement through VO2 measurement.

REFERENCES

[1] A. Dollar and H. Herr, "Lower extremity exoskeletons and active orthoses: Challenges and state-of-the-art," *IEEE Trans. Robot.*, vol. 24, no. 1, pp. 144–158, Feb. 2008.

[2] A. Dollar, H. Herr, R. Chatila, A. Kelly, and J. Merlet, "Design of a quasi-passive knee exoskeleton to assist running," in *Proc. 2008 IEEE/RSJ Int. Conf. Robots Intell. Syst.*, 2008, pp. 747–754.

[3] K. Shamaei, P. Napolitano, and A. Dollar, "A quasi-passive compliant stance control knee-ankle-foot orthosis," presented at the IEEE Int. Conf. Rehabil. Robot., Seattle, WA, USA, 2013.

[4] K. Gregorczyk, L. Hasselquist, J. Schiffman, C. Bensel, J. Obusek, and D. Gutekunst, "Effects of a lower-body exoskeleton device on metabolic cost and gait biomechanics during load carriage," *Ergonomics*, vol. 53, no. 10, pp. 1263–1275, 2010.

[5] R. Ronsse, T. Lenzi, N. Vitiello, B. Koopman, E. Van Asseldonk, S. De Rossi, J. Van den Kieboom, H. Van Der Kooij, M. Carrozza, and A. Ijspeert, "Oscillator-based assistance of cyclical movements: Model-based and model-free approaches," *Med. Biol. Eng. Comput.*, vol. 49, no. 10, pp. 1173–1185, 2011.

[6] C. Walsh, K. Endo, and H. Herr, "A quasi-passive leg exoskeleton for load-carrying augmentation," *Int. J. Humanoid Robot.*, vol. 4, no. 3, pp. 487–506, Sep. 2007.

[7] G. Sawicki, A. Domingo, and D. Ferris, "The effects of powered ankle-foot orthoses on joint kinematics and muscle activation during walking in individuals with incomplete spinal cord injury," *J. Neuroeng. Rehabil.*, vol. 3, pp. 1–17, Feb. 28, 2006.

[8] D. Ferris, Z. Bohra, J. Lukos, and C. Kinnaird, "Neuromechanical adaptation to hopping with an elastic ankle-foot orthosis," *J. Appl. Physiol.*, vol. 100, no. 1, pp. 163–170, Jan. 2006.

[9] D. Farris and G. Sawicki, "Linking the mechanics and energetics of hopping with elastic ankle exoskeletons," *J. Appl. Physiol.*, vol. 113, no. 12, pp. 1862–1872, Oct. 2012.

[10] A. Roy, H. Krebs, D. Williams, C. Bever, L. Forrester, R. Macko, and N. Hogan, "Robot-aided neurorehabilitation: A novel robot for ankle rehabilitation," *IEEE Trans. Robot.*, vol. 25, no. 3, pp. 569–582, Jun. 2009.

[11] A. Grabowski and H. Herr, "Leg exoskeleton reduces the metabolic cost of human hopping," *J. Appl. Physiol.*, vol. 107, no. 3, pp. 670–678, Sep. 2009.

[12] R. Gregg, T. Bretl, and M. Spong, "A control theoretic approach to robot-assisted locomotor therapy," in *Proc. 49th IEEE Conf. Decision Control*, 2010, pp. 1679–1686.

[13] M. Cherry, D. Choi, K. Deng, S. Kota, and D. Ferris, "Design and fabrication of an elastic knee orthosis: Preliminary results," in *Proc. IDETC/CIE ASME 2006 Int. Design Eng. Tech. Conf. Comput. Inform. Eng. Conf.*, Philadelphia, PA, USA, 2006, pp. 567–573.

[14] H. Kazerooni, R. Steger, and L. Huang, "Hybrid control of the Berkeley lower extremity exoskeleton (BLEEX)," *Int. J. Robot. Res.*, vol. 25, no. 5–6, pp. 561–573, May /Jun. 2006.

[15] G. Aguirre-Ollinger, J. Colgate, M. Peshkin, and A. Goswami, "Design of an active one-degree-of-freedom lower-limb exoskeleton with inertia compensation," *Int. J. Robot. Res.*, vol. 30, no. 4, pp. 486–499, Apr. 2011.

[16] M. Wehner, B. Quinlivan, P. Aubin, E. Martinez-Villalpando, M. Baumann, L. Stirling, K. Holt, R. Wood, and C. Walsh, "A lightweight soft exosuit for gait assistance," in *Proc. IEEE Int. Conf. Robot. Autom.*, 2013, pp. 3362–3369.

[17] P. Kao, C. Lewis, and D. Ferris, "Invariant ankle moment patterns when walking with and without a robotic ankle exoskeleton," *J. Biomechanics*, vol. 43, no. 2, pp. 203–209, Jan. 19, 2010.

[18] S. Agrawal, S. Banala, A. Fattah, V. Sangwan, V. Krishnamoorthy, J. Scholz, and W. Hsu, "Assessment of motion of a swing leg and gait rehabilitation with a gravity balancing exoskeleton," *IEEE Trans. Neural Syst. Rehabil. Eng.*, vol. 15, no. 3, pp. 410–420, Sep. 2007.

[19] G. Elliott, G. Sawicki, A. Marecki, and H. Herr, "The biomechanics and energetics of human running using an elastic knee exoskeleton," in *Proc. IEEE Conf. Rehabil. Robot.*, Seattle, WA, USA, 2013.

[20] K. Shamaei, M. Cenciarini, and A. Dollar, "On the mechanics of the ankle in the stance phase of the gait," in *Proc. IEEE Annu. Int. Conf. Eng. Med. Biol. Soc.*, Boston, MA, USA, 2011, pp. 8135–8140.

[21] K. Shamaei and A. Dollar, "On the mechanics of the knee during the stance phase of the gait," in *Proc. IEEE Int. Conf. Rehabil. Robot.*, Zurich, Switzerland, 2011, pp. 1–7.

[22] K. Shamaei, G. Sawicki, and A. Dollar, "Estimation of quasi-stiffness and propulsive work of the human ankle in the stance phase of walking," *PLoS One*, vol. 8, no. 3, pp. 1–12, 2013.

[23] K. Shamaei, G. Sawicki, and A. Dollar, "Estimation of quasi-stiffness of the human knee in the stance phase of walking," *PLoS One*, vol. 8, no. 3, pp. 1–10, 2013.

[24] M. Cenciarini and A. Dollar, "Biomechanical considerations in the design of lower limb exoskeletons," in *Proc. IEEE Int. Conf. Rehabil. Robot.*, Zurich, Switzerland, 2011, pp. 1–6.

[25] P. Kao, C. Lewis, and D. Ferris, "Short-term locomotor adaptation to a robotic ankle exoskeleton does not alter soleus Hoffmann reflex amplitude," *J. Neuroeng. Rehabil.*, vol. 7, no. 1, pp. 1–8, 2010.

[26] J. Sulzer, R. Roiz, M. Peshkin, and J. Patton, "A highly backdrivable, lightweight knee actuator for investigating gait in stroke," *IEEE Trans. Robot.*, vol. 25, no. 3, pp. 539–548, Jun. 2009.

[27] M. Noel, K. Fortin, and L. Bouyer, "Using an electrohydraulic ankle foot orthosis to study modifications in feedforward control during locomotor adaptation to force fields applied in stance," *J. Neuroeng. Rehabil.*, vol. 6, no. 1, pp. 1–11, 2009.

[28] A. Roy, H. Krebs, S. Patterson, T. Judkins, I. Khanna, L. Forrester, R. Macko, and N. Hogan, "Measurement of human ankle stiffness using the anklebot," in *Proc. IEEE 10th Int. Conf. Rehabil. Robot.*, 2007, pp. 356–363.

[29] T. Lenzi, M. Carrozza, and S. Agrawal, "Powered hip exoskeletons can reduce the user's hip and ankle muscle activations during walking," *IEEE Trans. Neural Syst. Rehabil. Eng.*, vol. 21, no. 6, pp. 938–948, Nov. 2013.

[30] E. Rouse, R. Gregg, L. Hargrove, and J. Sensinger, "The difference between stiffness and quasi-stiffness in the context of biomechanical modeling," *IEEE Trans. Biomed. Eng.*, vol. 60, no. 2, pp. 562–568, 2013.

[31] C. Frigo, P. Crenna, and L. Jensen, "Moment-angle relationship at lower limb joints during human walking at different velocities," *J. Electromyography Kinesiology*, vol. 6, no. 3, pp. 177–190, Sep. 1996.

[32] K. Shamaei, G. S. Sawicki, and A. M. Dollar, "Estimation of quasi-stiffness of the human hip in the stance phase of walking," *PLoS One*, vol. 8, no. 12, pp. 1–11, 2013.

[33] J. Rose and J. Gamble, *Human Walking*. Philadelphia, PA, USA: Williams & Wilkins, 2006.

[34] D. Winter, *The Biomechanics and Motor Control of Human Gait: Normal, Elderly and Pathological.* 2nd ed., Waterloo, ON, Canada: Univ. Waterloo Press, 1991.

[35] J. Perry, *Gait Analysis : Normal and Pathological Function.* Thorofare, NJ, USA: Slack, 1992.

[36] R. Davis and P. DeLuca, "Gait characterization via dynamic joint stiffness," *Gait Posture*, vol. 4, no. 3, pp. 224–231, 1996.

[37] D. Stefanyshyn and B. Nigg, "Dynamic angular stiffness of the ankle joint during running and sprinting," *J. Appl. Biomechanics*, vol. 14, no. 3, pp. 292–299, Aug. 1998.

[38] P. Crenna and C. Frigo, "Dynamics of the ankle joint analyzed through moment-angle loops during human walking: gender and age effects," *Human Movement Sci.*, vol. 30, no. 6, pp. 1185–1198, 2011.

[39] S. Lark, J. Buckley, S. Bennett, D. Jones, and A. Sargeant, "Joint torques and dynamic joint stiffness in elderly and young men during stepping down," *Clin. Biomechanics*, vol. 18, no. 9, pp. 848–855, Nov. 2003.

[40] D. Ferris and C. Farley, "Interaction of leg stiffness and surface stiffness during human hopping," *J. Appl. Physiol.*, vol. 82, no. 1, pp. 15–22, Jan. 1997.

[41] C. Farley, H. Houdijk, C. Van Strien, and M. Louie, "Mechanism of leg stiffness adjustment for hopping on surfaces of different stiffnesses," *J. Appl. Physiol.*, vol. 85, no. 3, pp. 1044–1055, Sep. 1998.

[42] G. Tatarliev, "Design of a knee simulator for testing orthoses under unlimited gait cycles," *School of Engineering and Applied Science*, New Haven, CT, USA: Yale Univ., 2011.

[43] I. McClay and K. Manal, "Three-dimensional kinetic analysis of running: Significance of secondary planes of motion," *Med. Sci. Sports Exercise*, vol. 31, no. 11, pp. 1629–1637, Nov. 1999.

Kamran Shamaei (S'11) received the B.S. degree in mechanical engineering from the Iran University of Science and Technology, Tehran, Iran, in 2005, the M.S. degree in mechanical engineering from ETH, Zurich, Switzerland, in 2009. He is currently working toward the Ph.D. degree from the School of Engineering and Applied Science, Yale University, New Haven, CT, USA.

His current research interests include design and development of orthoses and prostheses, medical robotics, and surgical technologies.

Massimo Cenciarini (S'09–M'11) received the Laurea degree in biomedical and electronic engineering from the University of Bologna, Bologna, Italy, in 2001, and the Ph.D. degree in bioengineering from the University of Pittsburgh, Pittsburgh, PA, USA, in 2010.

He is currently a Postdoctoral Scientist in the Neurologische Universitätsklinik Freiburg, Freiburg, Germany, since May 2013. He was a Postdoctoral Associate with Dr. A. Dollar at Yale University, New Haven, CT, USA, working on lower limbs exoskeleton, orthosis, and leg biomechanics from November 2010–April 2013. His current research interests include modeling of human balance and locomotion with emphasis on identifying and characterize factors such as gender, aging, and neurological disorders to the control of balance.

Albert A. Adams received the Bachelor's degree in biomedical engineering from The Catholic University of America, Washington, DC, USA, where he worked with the National Rehabilitation Hospital to design rehabilitation robotics that aid stroke patients in recovering hand function. The M.S. degree in biomedical engineering from Worcester Polytechnic Institute, Worcester, MA, USA, he investigated how extremity armor affected Soldiers' physical performance.

Working for the U.S. Army since 2004, he has conducted biomechanics research ranging from the use of nonlinear mathematics to quantify the effects of prolonged load carriage to evaluating the effects of exoskeletons on gait.

Karen N. Gregorczyk received the B.A. degree in physics at the College of the Holy Cross, Worcester, MA, USA, and the M.S. degree in biomedical engineering from Worcester Polytechnic Institute, Worcester.

She is a Research Biomechanist and Principal Investigator at the Center for Military Biomechanics Research, U.S. Army Natick Soldier Research, Engineering, and Development Center. She has led and contributed to several key efforts and programs spanning from basic to applied research that focus on the biomechanical implications of wearing soldier equipment and exoskeletons designed to augment the soldier.

Jeffrey M. Schiffman received the Doctoral degree in biomechanics from the Department of Health, Sports, and Exercise Science, University of Kansas, Lawrence, KS, USA, in 1999.

Since 2010, he has been a Supervisory Research Physiologist at Natick Soldier Research, Development and Engineering Center (NSRDEC), Natick, MA, USA. He currently leads the Biomechanics Team research activities, which includes a portfolio representing basic and applied research that focus on optimizing biomechanical and physiological aspects of Soldier performance and load carriage.

Aaron M. Dollar (SM'13) received the B.S. degree in mechanical engineering from the University of Massachusetts at Amherst, Amherst, MA, USA, the S.M. and Ph.D. degrees in engineering sciences from Harvard University, Cambridge, MA.

He conducted two years of Postdoctoral Research at the MIT Media Lab. He is the John J. Lee Associate Professor of Mechanical Engineering and Materials Science at Yale. His research interests include human and robotic grasping and dexterous manipulation, mechanisms and machine design, and assistive and rehabilitation devices including upper-limb prosthetics and lower-limb orthoses.

Dr. Dollar received the 2013 DARPA Young Faculty Award, 2011 AFOSR Young Investigator Award, the 2010 Technology Review TR35 Young Innovator Award, and the 2010 NSF CAREER Award.